A New Computational Method for Quasi-TE Mode Effective Index in Rib Waveguides

CHIN-SUNG HSIAO*
Department of Computer and Communication, Asia University, Taiwan

ABSTRACT

In this paper, we propose a new numerical method for solving a rib waveguide TE-mode problem. In the proposed method, the cross-section of the waveguide is divided into several regions and the refractive index profile and field distribution in each region are expanded into Fourier cosine series, and then are substituted in the wave equation. A second-order differential matrix equation is derived with a closed-form solution obtainable. Finally, with the boundary conditions being used, an eigenmode equation can be derived and solved numerically to give the modal indices. Here, the proposed method is used to deal with a silicon dioxide based rib waveguide. Numerical results show that the presented method is quite efficient, in terms of CPU time, in finding the modal indices accurately. The relative error of the modal index with the proposed method as compared that of the commercial software BeamPROP is less than 10^{-6}.

Key words: fourier cosine series expansion, rib waveguide, eigenmode equation, closed-form solution, Newton-Raphson algorithm.

1. INTRODUCTION

For more than twenty years, many researchers have directed considerable effort to computing the mode index of optical waveguides, which are the important parts of photonic integrated circuits. Many kinds of numerical methods have been utilized for the computation of modal fields and the modal indices of a rib waveguide. These methods include finite difference method (Kriezis & Papagiannakis, 1995; Hadley & Smith, 1995; Noro & Nakayama, 1996; Lusse, Stuwe, Schule & Unger, 1994) finite element method (Rahman & Davis, 1985; Kawano & Kitoh 2001; Koshiba, Saitoh, Eguchi & Hirayama, 1992), beam propagation method (Yevick & Hermansson, 1989; Kriezis & Papagiannakis, 1995; Liu, Yang & Yuan, 1993; Huang, Xu, Chu & Chaudhuri, 1992) and many other semi-analytic methods (Berry, Burke, Smartt, Benson, & Kendall, 1995; Burke, 1989). Numerical methods based on finite element or finite difference basically discretize the transverse domain of an optical waveguide to induce an eigenvalue problem.

In this paper, a new numerical approach is proposed to calculate the modal indices and modal fields of a quasi-TE mode of optical rib waveguides. In the method, the cross section of a rib waveguide is separated into four regions, in each of which, both the refractive index profile and the field distribution are represented as Fourier cosine series, respectively. In each region, a solution form of modal

* E-mail: cshsiao@asia.edu.tw

fields can be derived from a second-order differential matrix equation. Similarly to other existing semi-analytic methods, the proposed method is quite efficient in computational time compared with the time-consuming finite-difference-based beam propagation method. The accuracy of finding the modal index depends on the number of terms used in expanding the aforementioned refractive profile (as well as the modal field) into Fourier cosine series. The method of expanding both refractive index profile and the field distribution into Fourier cosine series has proven to be relatively efficient and accurate in finding the modes of one-dimensional optical waveguides (Wang & Huang, 1999; Wang & Hsiao, 2001) (i.e., slab waveguides). This technique has been for the first time applied to optical rib waveguides here. Note that neither an effective rib waveguide nor mode expansion (for the rib region) is used by the proposed method. Furthermore, the index profile is expressed into a Fourier (cosine) series in each region and then substituted into the wave equation to obtain a corresponding matrix equation, from which an exact closed-form solution for the field can be found. The expansion of the field here is only one-dimensional and consequently results in N or M equations (not NxM equations as in the 2-D Fourier method (Henry & Verbeek, 1989)) to be solved. In Section two, the theory of the proposed matrix method is outlined for the cases of quasi-TE modes. The computational results are presented in Section three, where one can see the accuracy and efficiency the method provides. Finally, Section four concludes this paper.

2. THEORY

In this study the considered geometric structure of the optical rib waveguide is shown in Figure 1, where the width and height of the rib are denoted by w and h, respectively, and the thickness of the slab is represented by d. The refractive indices of the guiding, substrate and cover region in the structure are n_1, n_2 and n_3, respectively. It should be noted that application of the theory outlined here is not strictly the case as shown in Figure 1, where homogeneity in composition is assumed throughout the rib and the slab.

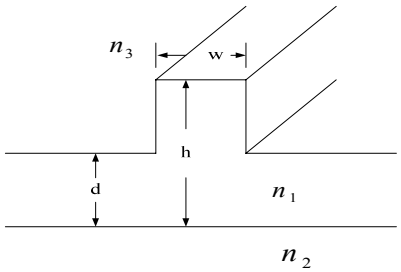

Figure 1. Geometric structure of the optical rib waveguide considered in this work. The refractive indices of the guiding region, substrate and cover are denoted by n_1, n_2 and n_3, respectively. w: rib's width, d: slab's thickness, h: height of the rib's top surface.

In the analysis of the quasi-TE mode of the rib waveguide, the cross-section of the considered waveguide is divided into four regions, as shown in Figure 2. The coordinates y_1 to y_3 represent, respectively, the boundaries between two corresponding adjacent regions. The coordinates x_1 and x_2 are the positions of the two rib's sidewalls. Clearly, for regions I (i.e., for $0 < y < y_1$), II ($y_1 < y < y_2$), and IV ($y_3 < y < y_4$), the refractive indices aren_2, n_1 and n_3 (all of which are constant), respectively; while for region III (i.e., for $y_2 < y < y_3$), the refractive index $n_0(x)$ follows the distribution

$$\begin{aligned} n_0^{\,2}(x) &= n_1^{\,2} \quad , \quad \text{for} \quad x_1 < x < x_2 \\ &= n_3^{\,2} \quad , \quad \text{for} \quad 0 < x < x_1 \quad \text{and} \quad x_2 < x < x_3 . \end{aligned} \tag{1}$$

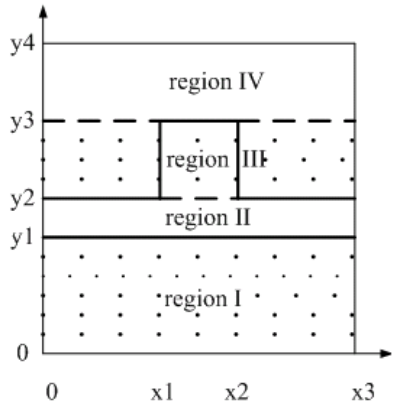

Figure 2. Dividing the cross-section of a rib waveguide into several regions in the cases of quasi-TE modes. y_1, y_2 and y_3 represent the coordinates in the y axis, denoting the interface between regions.

Note that the function $n_0^{\,2}(x)$ can be extended into an even periodic function with a period of $2*x_3$. Then we can have the Fourier cosine series expansion $n_0^{\,2}(x) = \sum_{n=0}^{N} a_n \cos n\Delta\omega x$ with $\Delta\omega = \pi / x_3$ and N being large enough. In each region defined in Figure 2, the magnetic field distribution can be expanded, i.e., we can write the field in region i as $H_i\,(x,y) = \sum_{n=0}^{N} h^i{}_n(y)\cos n\Delta\omega x$, a periodic distribution extended over $-\infty < x < \infty$. Here $h_n^{\,i}$ represents the amplitude of a spatial spectral component in the Fourier expansion for region i. Now we consider the quasi-TE modes wave equation

$$\frac{\partial^2 H_y}{\partial x^2} + \frac{\partial^2 H_y}{\partial y^2} - \frac{1}{n^2}\frac{\partial n^2}{\partial x}\frac{\partial H_y}{\partial x} + (k_0^{\,2} n^2 - \beta^2) H_y = 0 \tag{2}$$

n is the refractive index (a function of x and y) and β the propagation constant of a quasi-TE mode.

Equation (2) is solved for each of the four regions as indicated in Figure 2. Note that for regions I, II and IV, n^2 is constant and the term $\frac{1}{n^2}\frac{\partial n^2}{\partial x}$ is zero. Therefore for these regions, Equation (2) reduces to

$$\frac{\partial^2 H_y}{\partial x^2}+\frac{\partial^2 H_y}{\partial y^2}+(k_0{}^2\ n_i{}^2-\beta^2)H_y=0\ . \tag{3}$$

In solving Equation (3) for each of the three regions, we use the Fourier cosine series expansion $H_y=\sum_{n=0}^{N}h^i{}_n(y)\cos n\Delta\omega x$, where the superscript i denotes a specified region (i = 1, 2 and 4 for regions I, II and IV, respectively.). For each region Equation (3) then reduces to

$$-\sum_{n=0}^{N}h_n{}^i(n\Delta\omega)^2\cos n\Delta\omega x+\sum_{n=0}^{N}\frac{\partial h_n{}^i}{\partial y^2}\cos n\Delta\omega x+(k_0{}^2n_i{}^2-\beta^2)\sum_{n=0}^{N}h_n{}^i\cos n\Delta\omega x=0\ . \tag{4}$$

By equating all the coefficients of $\cos n\Delta\omega x$ (n = 0, 1, 2,….., N) in Equation (4) to zero, we obtain N+1 differential equations that can be expressed in a matrix form. For region I, the matrix equation turns out to be

$$\frac{\partial^2 H_1}{\partial y^2}+(k_0{}^2n_2{}^2I-W-\beta^2\mathrm{I})H_1=0\ . \tag{5}$$

The matrix equations for regions II and IV are, respectively,

$$\frac{\partial^2 H_2}{\partial y^2}+(k_0{}^2n_1{}^2I-W-\beta^2\mathrm{I})H_2=0\ ; \tag{6}$$

$$\frac{\partial^2 H_4}{\partial y^2}+(k_0{}^2n_3{}^2I-W-\beta^2\mathrm{I})H_4=0\ . \tag{7}$$

Here vectors H_1, H_2 and H_4 are defined by $H_1=[h_0{}^1,h_1{}^1,h_2{}^1,\cdots\cdots,h_N{}^1]^T$, $H_2=[h_0{}^2,h_1{}^2,h_2{}^2,\cdots\cdots,h_N{}^2]^T$ and $H_4=[h_0{}^4,h_1{}^4,h_2{}^4,\cdots\cdots,h_N{}^4]^T$, respectively.

To find H_y in region III, we note that n^2 is not homogeneous and we then use the Fourier cosine series expansion of n^2, i.e., $n^2=\sum_{n=0}^{N}a_n\cos n\Delta\omega x$. We can then put $n^2=\sum_{n=0}^{N}a_n\cos n\Delta\omega x$ and $H_y=\sum_{n=0}^{N}h^3{}_n(y)\cos n\Delta\omega x$ into Equation (2) to derive a differential matrix equation, i.e.,

$$\frac{\partial^2 H_3}{\partial y^2} + (k_0{}^2 A - W - P^{-1}Q - \beta^2 \mathrm{I})H_3 = 0 \tag{8}$$

where vector H_3 is given as $H_3 = [h_0{}^3, h_1{}^3, h_2{}^3, \cdots, h_N{}^3]^T$; matrix P is equal to 2 A; where matrix A and matrix Q are defined by

$$A = \frac{1}{2}\begin{bmatrix} 2a_0 & a_1 & a_2 & a_3 & \cdot\ \cdot & a_{N-1} & a_N \\ 2a_1 & 2a_0+a_2 & a_1+a_3 & a_2+a_4 & \cdot\ \cdot & a_{N-2}+a_N & a_{N-1}+a_{N+1} \\ 2a_2 & a_1+a_3 & 2a_0+a_4 & a_1+a_5 & \cdot\ \cdot & a_{N-3}+a_{N+1} & a_{N-2}+a_{N+2} \\ 2a_3 & a_2+a_4 & a_1+a_5 & 2a_0+a_6 & \cdot\ \cdot & \cdot & \cdot \\ \cdot & \cdot & \cdot & \cdot & \cdot\ \cdot & \cdot & \cdot \\ \cdot & \cdot & \cdot & \cdot & \cdot\ \cdot & \cdot & \cdot \\ \cdot & \cdot & \cdot & \cdot & \cdot\ \cdot & 2a_0+a_{2(N-1)} & \cdot \\ 2a_N & a_{N-1}+a_{N+1} & \cdot & \cdot & \cdot\ \cdot & \cdot & 2a_0+a_{2N} \end{bmatrix}; \tag{9}$$

$$Q = \begin{bmatrix} 0 & a_1(\Delta\omega)^2 & a_2(2\Delta\omega)^2 & a_3(3\Delta\omega)^2 & a_4(4\Delta\omega)^2 \\ 0 & 2a_2(\Delta\omega^2) & (a_1+a_3)2\Delta\omega^2 & (2a_2+4a_4)3\Delta\omega^2 & (3a_3+5a_5)4\Delta\omega^2 \\ 0 & (-a_1+3a_3)\Delta\omega^2 & 4a_4(2\Delta\omega^2) & (a_1+5a_5)3\Delta\omega^2 & (2a_2+6a_6)4\Delta\omega^2 \\ 0 & (-2a_2+4a_4)\Delta\omega^2 & (-a_1+5a_5)2\Delta\omega^2 & 6a_6(3\Delta\omega^2) & (1a_1+7a_7)4\Delta\omega^2 \\ 0 & (-3a_3+5a_5)\Delta\omega^2 & (-2a_2+6a_6)2\Delta\omega^2 & (-a_1+7a_7)3\Delta\omega^2 & 8a_8(4\Delta\omega^2) \\ \cdot & \cdot & \cdot & \cdot & \cdot \\ \cdot & \cdot & \cdot & \cdot & \cdot \\ \cdot & \cdot & \cdot & \cdot & \cdot \\ \cdot & \cdot & \cdot & \cdot & \cdot \\ 0 & (-3a_3+5a_5)\Delta\omega^2 & \cdot & \cdot & \cdot \end{bmatrix}$$

$$\begin{bmatrix} \cdot\ \cdot\ \cdot\ \cdot & a_N(N\Delta\omega)^2 \\ \cdot\ \cdot\ \cdot\ \cdot & [(N+1)a_{N+1}+(N-1)a_{N-1}]N\Delta\omega^2 \\ \cdot\ \cdot\ \cdot\ \cdot & [(N+2)a_{N+2}+(N-2)a_{N-2}]N\Delta\omega^2 \\ \cdot\ \cdot\ \cdot\ \cdot & [(N+3)a_{N+3}+(N-3)a_{N-3}]N\Delta\omega^2 \\ \cdot\ \cdot\ \cdot\ \cdot & \cdot \\ \cdot\ \cdot\ \cdot\ \cdot & \cdot \\ \cdot\ \cdot\ \cdot\ \cdot & \cdot \\ \cdot\ \cdot\ \cdot\ \cdot & \cdot \\ \cdot\ \cdot\ \cdot\ \cdot & \cdot \\ \cdot\ \cdot\ \cdot\ \cdot & 2Na_{2N}(N\Delta\omega^2) \end{bmatrix}. \tag{10}$$

The details of the derivation for Equation (8) are given in Appendix A.

Explicit solutions to Equations (5)-(8) can be written, respectively, as

$$H_1(y)=\begin{bmatrix} g_0\exp[\sqrt{\beta^2-\kappa_0}\,(y-y_1)] \\ g_1\exp[\sqrt{\beta^2-\kappa_1}\,(y-y_1)] \\ g_2\exp[\sqrt{\beta^2-\kappa_2}\,(y-y_1)] \\ . \\ . \\ . \\ g_N\exp[\sqrt{\beta^2-\kappa_N}\,(y-y_1)] \end{bmatrix}; \qquad H_2(y)=\begin{bmatrix} b_0\cos[\sqrt{\gamma_0-\beta^2}\,(y-y_1)-\phi_0] \\ b_1\cos[\sqrt{\gamma_1-\beta^2}\,(y-y_1)-\phi_1] \\ b_2\cos[\sqrt{\gamma_2-\beta^2}\,(y-y_1)-\phi_2] \\ . \\ . \\ . \\ b_N\cos[\sqrt{\gamma_N-\beta^2}\,(y-y_1)-\phi_N] \end{bmatrix};$$

$$H_4(y)=\begin{bmatrix} d_0\exp[-\sqrt{\beta^2-\delta_0}\,(y-y_3)] \\ d_1\exp[-\sqrt{\beta^2-\delta_1}\,(y-y_3)] \\ d_2\exp[-\sqrt{\beta^2-\delta_2}\,(y-y_3)] \\ . \\ . \\ . \\ d_N\exp[-\sqrt{\beta^2-\delta_N}\,(y-y_3)] \end{bmatrix} \quad \text{and} \quad H_3=\sum_{n=0}^{N}Y_n c_n\cos[\sqrt{\lambda_n-\beta^2}\,(y-y_2)-\theta_n)\,. \quad (11)$$

Here in this subsection κ_i, γ_i, λ_i, and δ_i (i = 0, 1, 2,….., N) are the eigenvalues of matrices $(k_0^{\,2}n_2^{\,2}I-W)$, $(k_0^{\,2}n_1^{\,2}I-W)$, $(k_0^{\,2}A-W-P^{-1}Q)$ and $(k_0^{\,2}n_3^{\,2}I-W)$, respectively; and $Y_i(i=0,1,2,\cdots\cdot,N)$ is the eigenvector of matrix $(k_0^{\,2}A-W-P^{-1}Q)$. The parameters $g_i s$, $b_i s$, $\phi_i s$, $d_i s$, $c_i s$, and $\theta_i s$ (i = 0, 1, 2,….., N) are all undetermined. They should, however, satisfy the boundary conditions at the interfaces $y = y_1$, $y = y_2$ and $y = y_3$. The boundary conditions for quasi-TE modes state that H_y and $\partial H_y \big/ \partial y$ are continuous at the interfaces. We have the following boundary conditions:

$$H_1(y_1)=H_2(y_1) \quad , \quad \frac{\partial H_1}{\partial y}\Big|y_1=\frac{\partial H_2}{\partial y}\Big|y_1\,;$$

$$H_2(y_2)=H_3(y_2) \quad , \quad \frac{\partial H_2}{\partial y}\Big|y_2=\frac{\partial H_3}{\partial y}\Big|y_2\,;$$

$$H_3(y_3)=H_4(y_3) \quad , \quad \frac{\partial H_3}{\partial y}\Big|y_3=\frac{\partial H_4}{\partial y}\Big|y_3\,. \quad (12)$$

Using the six boundary conditions above, we can derive two matrix identities as shown below.

$$K(\beta)\cdot X-L(\beta)\cdot Y=0\,; \quad (13)$$

$$M(\beta)\cdot X + N(\beta)\cdot Y = 0\,. \tag{14}$$

Here vectors X and Y are defined as

$$X = \begin{bmatrix} c_0\cos\theta_0 \\ c_1\cos\theta_1 \\ c_2\cos\theta_2 \\ \cdot \\ \cdot \\ \cdot \\ c_N\cos\theta_N \end{bmatrix} \quad \text{and} \quad Y = \begin{bmatrix} c_0\sin\theta_0 \\ c_1\sin\theta_1 \\ c_2\sin\theta_2 \\ \cdot \\ \cdot \\ \cdot \\ c_N\sin\theta_N \end{bmatrix}. \tag{15}$$

Matrices K, L, M and N contain elements that depend on β. The details for the derivations of Equations (13) and (14) and the definitions of K, L, M and N are given in Appendix A.

To solve for β, we rewrite Equations (13) and (14) as

$$\begin{bmatrix} K(\beta) & -L(\beta) \\ M(\beta) & N(\beta) \end{bmatrix}\cdot\begin{bmatrix} X \\ Y \end{bmatrix} = \begin{bmatrix} 0 \\ 0 \end{bmatrix}. \tag{16}$$

Since there should exist a nontrivial solution for Equation (16), the following equation must hold.

$$\det\left\{\begin{bmatrix} K(\beta) & -L(\beta) \\ M(\beta) & N(\beta) \end{bmatrix}\right\} = 0 \tag{17}$$

where $\det\{.\}$ represents the determinant of a matrix. The equation in (17) is thus used to determine the modal index (which is equal to β/k_0). A Newton-Raphson algorithm (Kublanovskaya, 1969) is quite efficient in solving Equation (17) and is used in this study. Once β is found, ϕ_i (i = 0, 1, 2,….., N) can be known (see Equation (A3) of Appendix A). Then b_i (i = 0, 1, 2,….., N) becomes propositional to g_i only (see Equation (A1)). From the equations in (A4) and (A5) of Appendix A, one can see that $c_i\cos\theta_i$ and $c_i\sin\theta_i$ depend on the coefficients $g_i s$ (i = 0, 1, 2,….., N). The parameter c_i and θ_i are both therefore a function of $g_i s$. The coefficients $d_i s$ are also dependent upon those $g_i s$ (i = 0, 1, 2,….., N), as can be clearly seen from Equation (A8) of Appendix A. In short summary, those $g_i s$ are independent variables, which all the parameters b_i, c_i, d_i, and θ_i are dependent upon. Therefore, all the vectors H_1, H_2, H_3 and H_4 (see Equation 11) can be determined given a set of $g_i s$ (i = 0, 1, 2,….., N). The field distribution of a quasi-TE mode can then be found.

3. NUMERICAL RESULTS

Here we present numerical results for one example of rib waveguide. The proposed method is used to calculate the modal index of a silicon dioxide based rib waveguide which is indicated as structure 1 listed in Table 1. This section also presents some results obtained by using the 2-D Fourier method (shown in the parenthesis in table 2). In using the 2-D Fourier method, we modeled the field as $\sum_{m=1}^{N}\sum_{n=1}^{N} e_{mn}\sin(m\Delta\omega x)\sin(n\Delta\omega y)$ and then obtained an eigenvalue equation, in which the order of the matrix is N^2. We ran the software BeamPROP, the 2-D Fourier method and the proposed method in the same PC with CPU 1.25MHZ.

Table 1. *The wavelength and the structural parameters of rib waveguide considered in this paper*

structure	λ	n1	n2	n3	w(μm)	h(μm)	d(μm)	x1(μm)	x3(μm)	y1(μm)	y4(μm)
1	1.55μm	1.46	1.45	1.45	5	5	2	23	51	12	29

The modal index of this single-mode waveguide for quasi-TE mode calculated by BeamPROP is 1.454667. The modal indices calculated by the proposed method are shown in Table 2. Comparisons between the results obtained by the proposed method and that obtained by BeamPROP can be seen in this table. Clearly, the n_{eff}s values calculated by the proposed method for N=38 are the same as the exact ones (which are obtained by BeamPROP). The CPU time for the proposed method is a fraction of a second to obtain such accurate results for quasi-TE mode. The 2-D Fourier method was also used to find the quasi-TE mode for this structure. The results for each N obtained by the 2-D Fourier method are shown in the parenthesis. Obviously, the 2-D Fourier method is quite time-consuming compared with the proposed method. The field distribution (for H_y) of the quasi-TE mode is shown by the contour drawn in Figure 3, where contour levels are at 10% intervals of the maximum field.

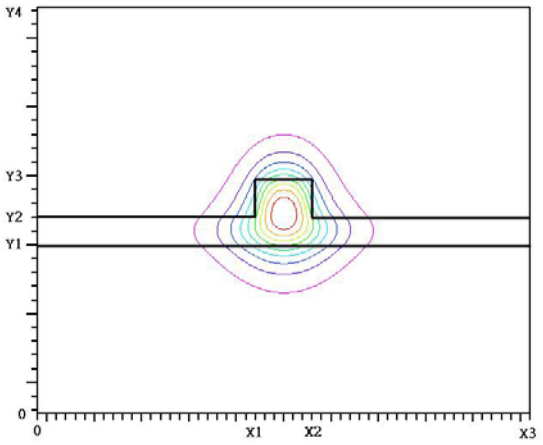

Figure 3. The field distribution (H_y) of the quasi-TE mode is shown by the contour, where contour levels are at 10% intervals of the maximum field.

Table 2. *Comparison of modal indices calculated by the proposed method, the 2-D Fourier method and the commercial software BeamPROP, for the quasi-TE mode of the rib waveguide of structure 1. For each N, the CPU time obtained by the 2-D Fourier method is shown in the parenthesis*

The proposed method			Beam PROP		
N	n_{eff}	cpu(sec)	grid sizes (μm)	n_{eff}	cpu(se`c)
10	1.454377	0.06(0.16)	$\Delta x = 0.5$, $\Delta y = 0.1$, $\Delta z = 10$	1.454657	0.8
15	1.454594	0.08(0.95)	$\Delta x = 0.25$, $\Delta y = 0.05$, $\Delta z = 5$	1.454665	7.5
20	1.454674	0.12(4.51)	$\Delta x = 0.125$, $\Delta y = 0.025$, $\Delta z = 5$	1.454667	27
25	1.454667	0.16(14.94)			
30	1.454662	0.23(38.56)			
32	1.454663	0.24(64.49)			
36	1.454666	0.27 (100.7)			
38	1.454667	0.28(140.56)			

4. CONCLUSIONS

Computing the mode index of the quasi-TE in optical rib waveguides is proposed in this paper. In the proposed method, we divide the cross-section of a rib waveguide into several regions and expand the modal field as well as the index profile into a Fourier cosine series; a second-order differential matrix equation for each region is then derived and a analytic solution form can then be readily found. By matching the continuity of the TE field at the interfaces between two adjacent regions, an eigenmode equation to be solved for modal indices is obtained. Numerical results demonstrate that the modal index can be found quite accurately and furthermore the CPU time spent in computation is much less than that when using the commercial software BeamPROP.

It is worth noting that the proposed method can also be applied to a SOI (silicon-on-insulator) rib-type waveguide coupler as shown in Figure 4(a), or a rib waveguide with multiple layers in the rib section as shown in Figure 4(b). The computation of the modal fields and modal indices for these other types of waveguides are based on the same analysis, in which the cross-section is divided into multiple regions and a second-order differential matrix equation is derived for each of them.

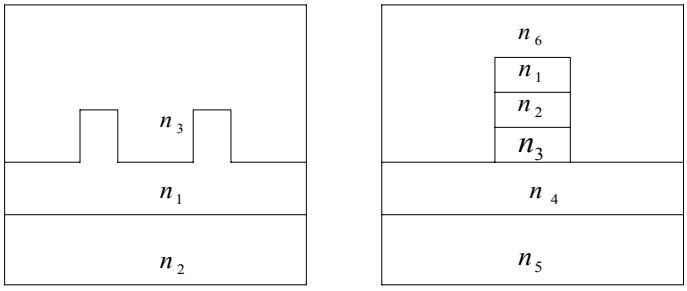

Figure 4. Cross-sections of (a) rib-type waveguide coupler and (b) rib waveguide with multiple layers in the rib section. Here n_i (i = 1, 2, 3, ….., 6) represents refractive index.

APPENDIX A

Here we derive Equations (13) and (14). The boundary condition $H_1(y_1) = H_2(y_1)$ leads to

$$g_i = b_i \cos\phi_i \qquad i = 0, 1, 2, \ldots, N \tag{A1}$$

while $H_1(y_1) = H_2(y_1)$ induces

$$g_i\sqrt{\beta^2 - \kappa_i} = b_i\sqrt{\gamma_i - \beta^2}\sin\phi_i \text{, for } i = 0, 1, 2, \ldots, N. \tag{A2}$$

Dividing (A2) by (A1), we obtain

$$\phi_i = \tan^{-1}\left[\sqrt{(\beta^2 - \kappa_i)\big/(\gamma_i - \beta^2)}\right] \text{, for } i = 0, 1, 2, \ldots, N. \tag{A3}$$

At the interface y_2, the boundary conditions $H_2(y_2) = H_3(y_2)$ and $H_2(y_2) = H_3(y_2)$ correspond to, respectively,

$$b_i \cos[\sqrt{\gamma_i - \beta^2}\,(y_2 - y_1) - \phi_i] = \sum_{n=0}^{N} Y_{ni} c_n \cos\theta_n \tag{A4}$$

and

$$-b_i\sqrt{\gamma_i - \beta^2}\sin[\sqrt{\gamma_i - \beta^2}\,(y_2 - y_1) - \phi_i] = \sum_{n=0}^{N}\sqrt{\lambda_n - \beta^2}\,Y_{ni} c_n \sin\theta_n$$

$$i = 0, 1, 2, \ldots, N. \tag{A5}$$

Equations (A5) and (A4) can combine to give (for $i = 0, 1, 2, \ldots, N$)

$$-\sqrt{\gamma_i - \beta^2}\tan[\sqrt{\gamma_i - \beta^2}\,(y_2 - y_1) - \phi_i]\cdot\sum_{n=0}^{N} Y_{ni} c_n \cos\theta_n = \sum_{n=0}^{N}\sqrt{\lambda_n - \beta^2}\,Y_{ni} c_n \sin\theta_{n\ i}. \tag{A6}$$

Y_{ni} ($i = 0, 1, 2, \ldots, N$) appearing above is the *i-th* element of vector Y_n as defined by $Y_n = [Y_{n0}, Y_{n1}, Y_{n2}, \ldots, Y_{nN}]^T$. The N+1 equations in (A6) can be put in a matrix form, i.e.,

$$\begin{bmatrix} K_{00} & K_{01} & \cdot & \cdot & \cdot & K_{0N} \\ K_{10} & K_{11} & \cdot & \cdot & \cdot & K_{1N} \\ K_{20} & K_{21} & \cdot & \cdot & \cdot & K_{2N} \\ \cdot & \cdot & \cdot & \cdot & \cdot & \cdot \\ \cdot & \cdot & \cdot & \cdot & \cdot & \cdot \\ \cdot & \cdot & \cdot & \cdot & \cdot & \cdot \\ K_{N0} & K_{N1} & \cdot & \cdot & \cdot & K_{NN} \end{bmatrix} \begin{bmatrix} c_0 \cos\theta_0 \\ c_1 \cos\theta_1 \\ c_2 \cos\theta_2 \\ \cdot \\ \cdot \\ \cdot \\ c_N \cos\theta_N \end{bmatrix} = \begin{bmatrix} L_{00} & L_{01} & \cdot & \cdot & \cdot & L_{0N} \\ L_{10} & L_{11} & \cdot & \cdot & \cdot & L_{1N} \\ L_{20} & L_{21} & \cdot & \cdot & \cdot & L_{2N} \\ \cdot & \cdot & \cdot & \cdot & \cdot & \cdot \\ \cdot & \cdot & \cdot & \cdot & \cdot & \cdot \\ \cdot & \cdot & \cdot & \cdot & \cdot & \cdot \\ L_{N0} & L_{N1} & \cdot & \cdot & \cdot & L_{NN} \end{bmatrix} \begin{bmatrix} c_0 \sin\theta_0 \\ c_1 \sin\theta_1 \\ c_2 \sin\theta_2 \\ \cdot \\ \cdot \\ \cdot \\ c_N \sin\theta_N \end{bmatrix} \tag{A7}$$

where K_{ij} and L_{ij} ($i, j = 0, 1, 2, \ldots, N$) are given by $K_{ij} = Y_{ji}\sqrt{\gamma_i - \beta^2}\tan[\sqrt{\gamma_i - \beta^2}(y_2 - y_1) - \phi_i]$ and $L_{ij} = Y_{ji}\sqrt{\lambda_i - \beta^2}$, respectively. Note that ϕ_i is a function of β.

The boundary conditions $H_3(y_3) = H_4(y_3)$ and $H_3(y_3) = H_4(y_3)$ induce the following set of equations:

$$\sum_{n=0}^{N} Y_{ni} c_n \cos[\sqrt{\lambda_n - \beta^2}(y_3 - y_2) - \theta_n] = d_i\,; \tag{A8}$$

$$\sum_{n=0}^{N} Y_{ni}\sqrt{\lambda_n - \beta^2} c_n \sin[\sqrt{\lambda_n - \beta^2}(y_3 - y_2) - \theta_n] = \sqrt{\beta^2 - \delta_i} d_i \quad i = 0, 1, 2, \ldots, N. \tag{A9}$$

By substituting d_i of (A8) in (A9), we obtain

$$\sum_{n=0}^{N} Y_{ni}\sqrt{\lambda_n - \beta^2} c_n \sin[\sqrt{\lambda_n - \beta^2}(y_3 - y_2) - \theta_n] = \sqrt{\beta^2 - \delta_i}\sum_{n=0}^{N} Y_{ni} c_n \cos[\sqrt{\lambda_n - \beta^2}(y_3 - y_2) - \theta_n]\,. \tag{A10}$$

The N+1 equations in (A10) can be rewritten in a matrix form, i.e.,

$$\begin{bmatrix} M_{00} & M_{01} & \cdot & \cdot & \cdot & M_{0N} \\ M_{10} & M_{11} & \cdot & \cdot & \cdot & M_{1N} \\ M_{20} & M_{21} & \cdot & \cdot & \cdot & M_{2N} \\ \cdot & \cdot & \cdot & \cdot & \cdot & \cdot \\ \cdot & \cdot & \cdot & \cdot & \cdot & \cdot \\ \cdot & \cdot & \cdot & \cdot & \cdot & \cdot \\ M_{N0} & M_{N1} & \cdot & \cdot & \cdot & M_{NN} \end{bmatrix} \begin{bmatrix} c_0 \cos\theta_0 \\ c_1 \cos\theta_1 \\ c_2 \cos\theta_2 \\ \cdot \\ \cdot \\ \cdot \\ c_N \cos\theta_N \end{bmatrix} + \begin{bmatrix} N_{00} & N_{01} & \cdot & \cdot & \cdot & N_{0N} \\ N_{10} & N_{11} & \cdot & \cdot & \cdot & N_{1N} \\ N_{20} & N_{21} & \cdot & \cdot & \cdot & N_{2N} \\ \cdot & \cdot & \cdot & \cdot & \cdot & \cdot \\ \cdot & \cdot & \cdot & \cdot & \cdot & \cdot \\ \cdot & \cdot & \cdot & \cdot & \cdot & \cdot \\ N_{N0} & N_{N1} & \cdot & \cdot & \cdot & N_{NN} \end{bmatrix} \begin{bmatrix} c_0 \sin\theta_0 \\ c_1 \sin\theta_1 \\ c_2 \sin\theta_2 \\ \cdot \\ \cdot \\ \cdot \\ c_N \sin\theta_N \end{bmatrix} = 0\,. \tag{A11}$$

Here M_{ij} and N_{ij} ($i, j = 0, 1, 2, \ldots, N$) are defined by

$M_{ij} = Y_{ji}\sqrt{\beta^2 - \delta_i}\cos[\sqrt{\lambda_j - \beta^2}(y_3 - y_2)]$ and $N_{ij} = Y_{ji}\sqrt{\beta^2 - \delta_i}\sin[\sqrt{\lambda_j - \beta^2}(y_3 - y_2)]$, respectively.

In deriving Equation (A11), we have used the identities cos(*x*-*y*) = cos*x*cos*y* + sin*x*sin*y* and sin(*x*-*y*) = sin*x*cos*y* - cos*x*sin*y* in Equation (A10). Equations (A7) and (A11) are further put in a simplified form, i.e.,

$$\begin{bmatrix} K(\beta) & -L(\beta) \\ M(\beta) & N(\beta) \end{bmatrix} \cdot \begin{bmatrix} X \\ Y \end{bmatrix} = \begin{bmatrix} 0 \\ 0 \end{bmatrix}$$

where the definitions of X and Y are given in Equation (14), while the definitions of submatrices $K(\beta)$, $L(\beta)$, $M(\beta)$ and $N(\beta)$ are self-evident by referring to Equations (A7) and (A11).

To derive Equation (8) from Equation (2), we define

$$\varphi(x, y) = \frac{1}{n^2}\frac{\partial n^2}{\partial x}\frac{\partial H_y}{\partial x} = \sum_{n=0}^{N}\phi_n(y)\cos n\Delta\omega x . \tag{A12}$$

From the definitions of Fourier cosine series expansions for n^2 and H_y, we have

$$\frac{\partial n^2}{\partial x} = -\sum_{n=0}^{N} n\Delta\omega \cdot a_n \sin n\Delta\omega x \tag{A13}$$

and

$$\frac{\partial H_y}{\partial x} = -\sum_{n=0}^{N} n\Delta\omega \cdot h_n{}^3(y)\sin n\Delta\omega x . \tag{A14}$$

From Equation (A12), which gives the identity $\varphi(x, y)\cdot n^2 = \frac{\partial n^2}{\partial x}\cdot\frac{\partial H_y}{\partial x}$, we obtain

$$\sum_{n=0}^{N}\phi_n(y)\cos n\Delta\omega x \cdot \sum_{n=0}^{N} a_n \cos n\Delta\omega x = (\sum_{n=0}^{N} n\Delta\omega a_n \sin n\Delta\omega x)\cdot(\sum_{n=0}^{N} n\Delta\omega h_n{}^3(y)\sin n\Delta\omega x) . \tag{A15}$$

Note that the double cosine/sine terms on both sides of Equation (A15) can reduce to cosine terms.

By equating all the coefficients of the cosine terms that have the same spatial frequency on both sides, we obtain a set of equations that can be put in the matrix form

$$P\phi(y) = QH_3 \tag{A16}$$

i.e.,

$$\phi(y) = P^{-1}QH_3 \tag{A17}$$

where matrices P and Q have been defined in Equation 9 and Equation 10; vector $\phi(y)$ is defined by $\phi(y) = [\phi_0(y), \phi_1(y), \phi_2(y), \cdots\cdots, \phi_N(y)]^T$.

Substituting the Fourier cosine series of H_y and φ in Equation (2), we then obtain

$$\sum_{n=0}^{N} \frac{\partial^2 h_n{}^3}{\partial y^2}(y)\cos n\Delta\omega x - \sum_{n=0}^{N}(n\Delta\omega)^2 h_n{}^3(y)\cos n\Delta\omega x - \sum_{n=0}^{N}\phi_n(y)\cos n\Delta\omega x +$$

$$k_0{}^2 \sum_{n=0}^{N}\sum_{m=0}^{N} a_n h_n{}^3(y)[\cos((m+n)\Delta\omega x) + \cos((m-n)\Delta\omega x)] - \beta^2 \sum_{n=0}^{N} h_n{}^3(y)\cos n\Delta\omega x = 0 \,. \tag{A18}$$

By collecting the coefficient of $\cos n\Delta\omega x$ for each n (n = 0, 1, 2, ….., N) and equating it to zero, we can have an N+1 differential equations that can be written in the matrix form

$$\frac{\partial^2 H_3}{\partial y^2} + (k_0{}^2 A - W - P^{-1}Q - \beta^2 \mathrm{I})H_3 = 0 \,. \tag{A19}$$

Here we have used Equation (A17) in deriving Equation (A19).

REFERENCES

Berry, G. M., Burke, S. V., Smartt, C. J., Benson, T. M., &. Kendall, P. C. (1995). Exact and variational Fourier transform methods for analysis of multilayered planar waveguides. *IEE J. Proc.-Optoelectron.*, *142*(1), 66-75.

Burke, S. V. (1989). Spectral index method applied to coupled rib waveguides. *Electronics Lett.*, *25*, 605-606.

Hadley, G. R., & Smith, R. E. (1995). Full-vector waveguide modeling using an iterative finite-difference method with transparent boundary conditions. *IEEE J. Lightwave Technol.*, *13*(3), 465-469.

Henry, C. H., & Verbeek, B. H. (1989). Solution of the scalar wave equation for arbitrarily shaped dielectric waveguides by two-dimensional Fourier analysis. *J. Lightwave Technol.*, *7*, 308-313.

Huang. W., Xu, C., Chu, S. T., & Chaudhuri, S. K. (1992). The finite-difference vector beam propagation method: analysis and assessment. *IEEE J. Lightwave Technol.*, *10*, 295-305.

Kawano, K., & Kitoh, T. (2001). *Introduction to optical waveguide analysis*. New York, USA: Wiley-Interscience.

Koshiba, M., Saitoh, H., Eguchi, M., & Hirayama, K. (1992). Simple scalar finite element approach to optical rib waveguides. *IEE J. Proc. J*, *139*, 166-171.

Kriezis, E. E., & Papagiannakis, A. G. (1995). A joint finite-difference and FFT full vectorial beam propagation scheme. *IEEE J. Lightwave Technol.*, *13*, 692-700.

Kublanovskaya, V. N. (1969). On an application of Newton's method to the determination of eigenvalues of λ-matrices. *Soviet Math. Dokl.*, *10*, 1240-1241.

Liu, P. L., Yang, S. L., & Yuan, D. M. (1993). The semivectorial beam propagation method. *IEEE J. Quantum Electron.*, *29*, 2639-2644.

Lusse, P., Stuwe, P., Schule, J., & Unger, H. G. (1994). Analysis of vectorial mode fields in optical waveguides by a new finite difference method. *IEEE J. Lightwave Technol.*, *12*(3), 487-493.

Noro, H., & Nakayama, T. (1996). A new approach to scalar and semivector mode analysis of optical waveguides. *IEEE J. Lightwave Technol.*, *14*(6), 1546-1556.

Rahman, B. M. A., & Davies, J. B. (1985). Vector-H finite element solution of GaAs/GaAlAs rib waveguides. *IEE J. Proc. J*, *l*(132), 349-353.

Wang, L., & Hsiao, C. S. (2001). A matrix method for studying TM modes of optical planar waveguides with arbitrary index profiles. *IEEE J. of Quantum Electron*, *37*, 1654-1660.

Wang, L., & Huang, N. (1999). A new numerical method for solving planar waveguide problems with arbitrary index profiles: TE mode solutions. *IEEE J. of Quantum Electron*, *35*, 1351-1353.

Yevick, D., & Hermansson, B. (1989). New formulations of the matrix beam propagation method: application to rib waveguides. *IEEE J. Quantum Electron.*, *25*(2), 221-229.

Chin-sung Hsiao received the B.S degree from National Taiwan University of Science and Technology, Taipei, Taiwan, R.O.C, and the M.S. degree from the University of Alabama, U.S.A, and his Ph.D degree from National Tsing Hua University, Hsinchu, Taiwan, respectively, all in electrical engineering.

In 1984, he joined TRW_{ECC} as a test engineer. In 1987, he joined USI Inc. as a thick-film circuit supervisor for communication products. He served at Hsiuping Institute of Technology from 1991 to 2005. He then joined Asia University, where he is currently an Associate Professor of the Department of Computer and Communication. His research interests include optical fiber communication, optical device design and numerical computation, communication theory and system, digital signal and digital image processing, fiber gratings and their applications.